PNAS RESEARCH ARTICLE | DEVELOPMENTAL BIOLOGY OPEN ACCESS

Comparative genomics of mortal and immortal cnidarians unveils novel keys behind rejuvenation

Maria Pascual-Torner[a,b,1,2], Dido Carrero[a,2], José G. Pérez-Silva[a], Diana Álvarez-Puente[a], David Roiz-Valle[a], Gabriel Bretones[a], David Rodríguez[a], Daniel Maeso[a], Elena Mateo-González[b], Yaiza Español[a], Guillermo Mariño[c,d], José Luis Acuña[b], Víctor Quesada[a,1], and Carlos López-Otín[a]

Edited by Vera Gorbunova, University of Rochester; received October 13, 2021; accepted July 6, 2022 by Editorial Board Member Helen M. Blau

Turritopsis dohrnii **is the only metazoan able to rejuvenate repeatedly after its medusae reproduce, hinting at biological immortality and challenging our understanding of aging. We present and compare whole-genome assemblies of *T. dohrnii* and the nonimmortal *Turritopsis rubra* using automatic and manual annotations, together with the transcriptome of life cycle reversal (LCR) process of *T. dohrnii*. We have identified variants and expansions of genes associated with replication, DNA repair, telomere maintenance, redox environment, stem cell population, and intercellular communication. Moreover, we have found silencing of polycomb repressive complex 2 targets and activation of pluripotency targets during LCR, which points to these transcription factors as pluripotency inducers in *T. dohrnii*. Accordingly, we propose these factors as key elements in the ability of *T. dohrnii* to undergo rejuvenation.**

aging | reprogramming | polycomb | pluripotency | *Turritopsis*

Natural selection declines with age and particularly affects genes that are important in prereproductive phenotypes, regardless of their postreproductive effects. Thus, variants that are damaging only late in life are not readily eliminated from the gene pool (1). Consequently, aging has evolved over time through modulation of traits related to the hallmarks of health (2) or to the determinants of aging, such as cellular senescence or genomic instability, which impair pluripotency and regeneration potentials (3). Several cnidarian species have challenged some of these traits and stand out for their singular developmental plasticity and even ontogeny reversals, while still sharing genomic structural features and pivotal genes with bilaterians (4–6).

Ontogeny reversal occurs in some cnidarian species (7, 8), but this ability is usually lost once individuals reach sexual maturity. Only three species within the genera *Turritopsis* have been reported to rejuvenate after reproduction: *Turritopsis dohrnii*, *Turritopsis* sp.5, and *Turritopsis* sp.2 (9). However, while the latter two sharply drop their reversal capacity after reaching maturity, *T. dohrnii* is the only one that maintains its high rejuvenation potential (up to 100%) in postreproductive stages, reaching biological immortality (10, 11).

In this study, we have sequenced the genomes of *T. dohrnii* and *T. rubra*, a closely related species without reported evidence of postreproductive rejuvenation (9) (Fig. 1), and used comparative genomic analyses to identify differential gene variants and amplifications between both species, as well as between them and the cnidarians *Hydra vulgaris*, *Clytia hemisphaerica*, and *Aurelia aurita*. The supervised and unsupervised comparison of genes involved in aging and DNA repair, together with the transcriptome analysis of life cycle reversal (LCR) of *T. dohrnii* have provided new insights into the molecular mechanisms underlying *Turritopsis* plasticity, which may contribute to the immortal phenotype of *T. dohrnii*.

Results and Discussion

The genomes of both species of *Turritopsis* were sequenced using the Illumina platform (*SI Appendix*, section 2.2) and assembled into a genome with an estimated size of 390 megabases (Mb) in *T. dohrnii*, which is consistent with previous estimates (genome size = 383 ± 4.84 Mb) (12), and 210 Mb in *T. rubra*. The assemblies of *T. dohrnii* and *T. rubra* contain 74,829 and 9,508 scaffolds, respectively, with N50 values of 10,419 and 71,856 kb. The quality of both assemblies, measured with Benchmarking sets of Universal Single-Copy Orthologs (BUSCO), indicates coverages of 78.88% and 88.78%, respectively (*SI Appendix*, section 3.1 and Table S1).

Automatic annotation using MAKER predicted a set of 17,468 genes in *T. dohrnii* and 9,324 genes in *T. rubra*. This difference in number of genes among *Turritopsis*

Significance

While aging affects most living organisms, the hydrozoan *Turritopsis dohrnii* is the only species able to rejuvenate repeatedly after sexual reproduction, becoming biologically immortal. Setting the whole-genome of this metazoan is indispensable to study in depth mechanisms responsible for its immortal phenotype. Here, we report the genome assembly of *T. dohrnii* and its congeneric species *Turritopsis rubra*, incapable of rejuvenating at mature stages. Further, we compare a set of almost 1,000 genes related to aging and DNA repair between both *Turritopsis* and other cnidarians and present a stage-specific transcriptome of life cycle reversal process of *T. dohrnii*. Altogether, these results unveil key molecular mechanisms behind rejuvenation of *T. dohrnii*.

Author affiliations: [a]Departamento de Bioquímica y Biología Molecular, Instituto Universitario de Oncología, Ciberonc, Universidad de Oviedo, Oviedo, 33006, Spain; [b]Observatorio Marino de Asturias, Departamento de Biología de Organismos y Sistemas, Universidad de Oviedo, Oviedo, 33006, Spain; [c]Departamento de Biología Funcional, Facultad de Medicina, Universidad de Oviedo, Oviedo, 33006, Spain; and [d]Autophagy and Metabolism Lab, Instituto de Investigación Sanitaria del Principado de Asturias (ISPA), Oviedo, 33011, Spain

The authors declare no competing interest.

This article is a PNAS Direct Submission. V.G. is a guest editor invited by the Editorial Board.

[1]To whom correspondence may be addressed. Email: mariapascual1.618@gmail.com or quesadavictor@uniovi.es.

[2]M.P.-T. and D.C. contributed equally to this work.

This article contains supporting information online at http://www.pnas.org/lookup/suppl/doi:10.1073/pnas.2118763119/-/DCSupplemental.

Published August 29, 2022.

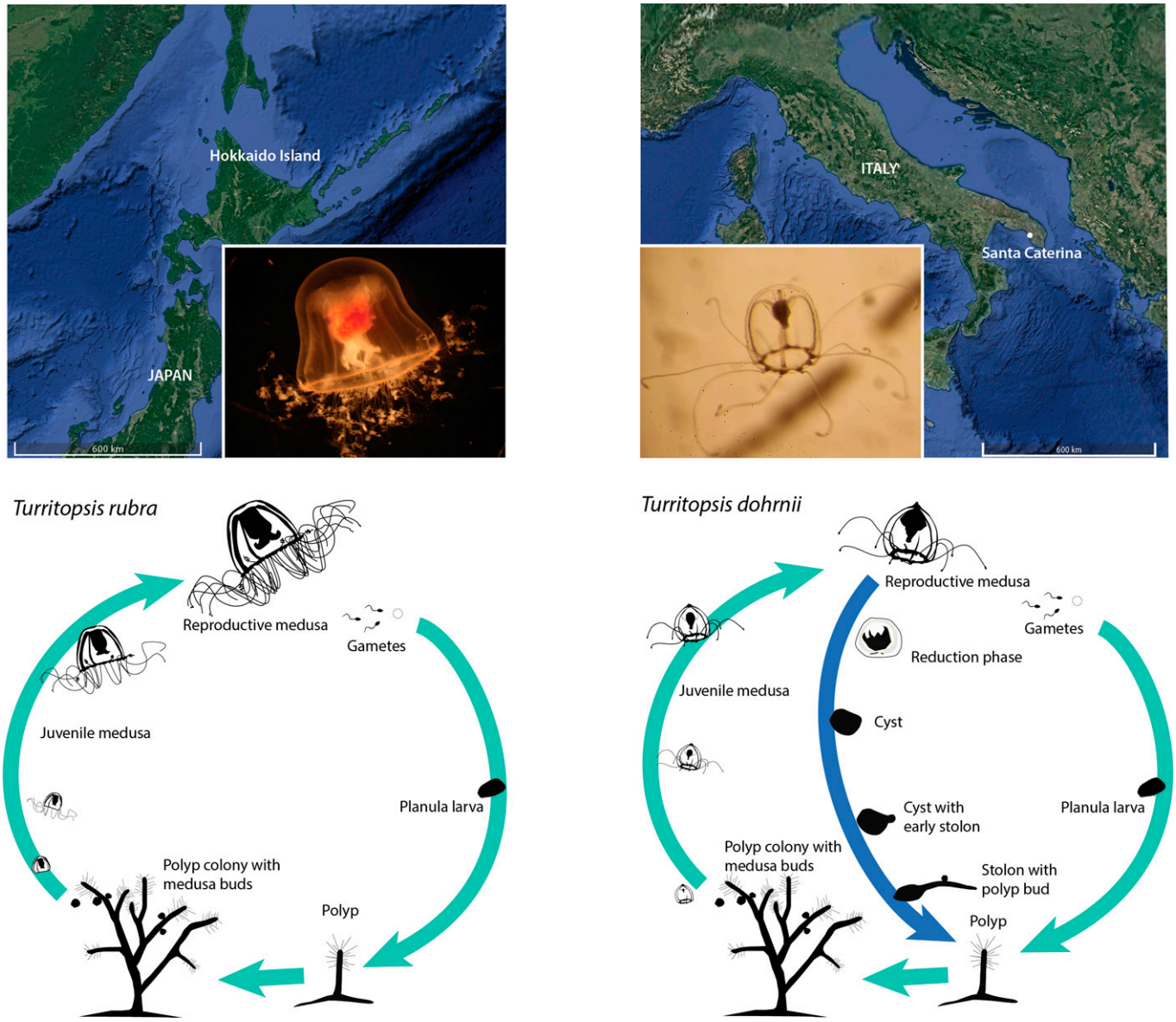

Fig. 1. Geographical origin and life cycle diagram of *T. rubra* (*Left*) and *T. dohrnii* (*Right*). Light blue arrows indicate the typical life cycle while dark blue indicates the alternative ontogeny reversal of *T. dohrnii*. In this process, the free swimming medusa shrinks until the cyst stage, where all structures from the medusa totally disappear into a homogeneous opaque mass. Later, a stolon starts growing from the cyst and polyp buds appear to become fully grown polyps afterward.

species is consistent with their genome sizes and, possibly, with the higher fragmentation in *T. dohrnii* (*SI Appendix*, sections 3.1 and 3.2 and Tables S1 and S2). Repetitive elements represent around half of the genome, similar to other cnidarian genomes (5, 6), and, although most of them were unclassified, long interspersed nuclear element and long terminal repeats were the most abundant retroelements (*SI Appendix*, Table S3). Together with automatic annotation, we used manual annotation to compare almost 1,000 genes involved in aging, DNA repair, and pathways of interest selected from a previously available LCR transcriptome of *T. dohrnii* (11) (*SI Appendix*, section 2.4 and Fig. S1 and Dataset S1). Previous whole-genome analysis projects have shown that this laborious but exhaustive annotation method is effective for the purpose of identifying gene amplifications and residue variants (13, 14). Specifically, we focused on variants affecting known motifs, truncating variants and variants related to genetic diseases in humans that were only present in one of the *Turritopsis* species. These variant and amplification candidates were further compared to the available genomes of 11 cnidarian species and, when still specific, they were validated with RNA-seq data, through examination of supporting genomic DNA reads, and by PCR amplification followed by Sanger sequencing (*SI Appendix*, sections 2.5 and 2.6). We identified 28 copy number variations and 10 variants unique for *T. dohrnii* or *T. rubra,* which were then classified into the 9 hallmarks of aging (3), depending on the affected genes (Fig. 2 and *SI Appendix*, section 3.3 and Fig. S3 and Tables S4–S9).

Considering their difference in genome size and number of genes, we would expect to find more amplified genes in *T. dohrnii* than in *T. rubra*. However, we found that the percentage of amplifications (genes with two or more copies) observed in *T. dohrnii* from our manually annotated list was 3.77 times higher than the one we obtained from a representative gene set of the whole genome in this species (a random set of 1,000 automatically annotated genes) (*SI Appendix*, section 3.3 and Table S10 and Fig. S4).

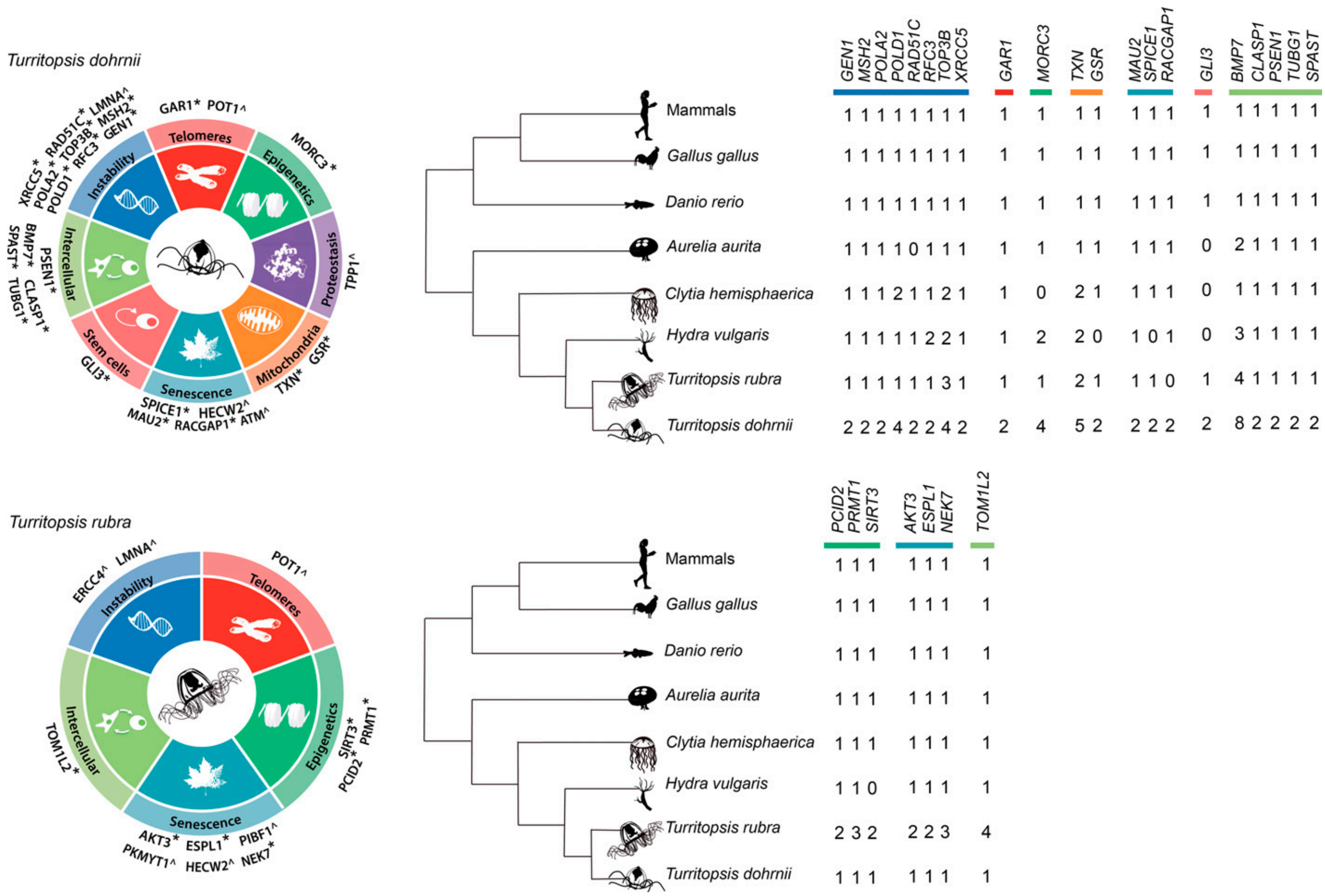

Fig. 2. Genomic basis of longevity in *Turritopsis*. Genes potentially implicated in cellular plasticity in *T. dohrnii* (*Top*) and *T. rubra* (*Bottom*) classified according to their putative role in the different hallmarks of aging. * indicates genes with copy number variations, while ^ refers to genes with point variants of interest.

Therefore, the differential increase in gene copies highlighted in this study is likely due to sporadic genetic events with positive selection or neutral processes rather than to a global mechanism of genomic expansion.

We were concerned that an important limitation of this work is the relative low quality of both assemblies and whether the higher number of copies found in *T. dohrnii* was an artifact of the greater fragmentation of its assembly. To face this limitation, we have used a very conservative and rigorous protocol during manual annotation: on the one hand, gene amplifications were only reported when two or more independent protein sequences overlapped the same sequence of the corresponding human orthologs (we considered only BLAST hits with e-value lower than 0.001). Otherwise, they were considered as parts of the same copy; on the other hand, the oligonucleotides used to perform PCR validations were carefully designed to be specific of each copy and have proved to be effective to differentiate independent gene copies (*SI Appendix*, Fig. S3 and Table S9). Successful PCRs (with a resulting gel band) indicated positive validation of the specific gene copy, while negative results prevented us from reaching any definitive conclusions and were consequently discarded (*SI Appendix*, Table S6). In that way, we were able to rule out candidate gene copies found manually that may result from fragmentation and assembly errors. Additionally, most copies were also supported by RNA-seq data, which reinforces their legitimacy (*SI Appendix*, Table S4).

The conclusions of this study are limited by the phylogenetic distance between *T. dohrnii* and *T. rubra* (9), as background differences unrelated to immortality are expected. Therefore, obtaining and analyzing material from a closer mortal congeneric species, such as *T. nutricula*, will be important to confirm and refine the interpretation of our results. It is also noteworthy that we define *T. dohrnii* as "immortal" because the probability of sexually mature medusae to rejuvenate goes up to 100%, with no apparent limit in the number of ontogeny reversal cycles for a given individual (10). In contrast, we consider *T. rubra* as "mortal" since we found no published evidence of postreproductive rejuvenation in this species (9). Following this premise, we suggest that *T. dohrnii* would have a set of mechanisms such as the ones found in this study that function synergically as a whole to warrant high organismal rejuvenation success even after reproduction, and that most of these mechanisms would be lacking in *T. rubra*.

Since genomic instability plays a major role in the regulation of aging, we analyzed a series of genes involved in DNA replication and repair. In this context, our results suggest that *T. dohrnii* may have more efficient replicative mechanisms and repair systems than the other cnidarians included in this study (*SI Appendix*, section 3.3.1). For instance, the amplifications of *POLD1* (encoding DNA polymerase delta) and *POLA2* (encoding DNA polymerase alpha 2) in *T. dohrnii* (four and two copies, respectively, compared to one in *T. rubra*) suggest enhanced replicative capabilities in this species. We also detected a duplication of *RFC3* (replication factor C 3) in *T. dohrnii and H. vulgaris*, as well as four copies of *TOP3B* (DNA topoisomerase III beta) in *T. dohrnii*, in comparison to three copies in *T. rubra*. Regarding DNA repair, we found duplications in *XRCC5* (X-ray

repair cross complementing 5), *GEN1* (gene endonuclease homolog 1), *RAD51C* (RAD51 paralog C) and *MSH2* (MUTS homolog 2) in *T. dohrnii* compared to the presence of one copy of these genes in *T. rubra*. We also detected two variants in highly conserved positions of *LMNA* (lamin A/C), p.G523A in *T. dohrnrii* and p.E82Q in *T. rubra* (*SI Appendix*, section 3.3.8 and Table S5 and Fig. S5). The copies of most of the abovementioned genes (except *GEN1* and one copy of *POLD1* and *TOP3B*) were transcriptionally active during LCR of *T. dohrnii*, which reinforces our hypothesis that more efficient replication and repair systems could underlie rejuvenation in this species (*SI Appendix*, Fig. S5).

Oxidative stress resulting from reactive oxygen species can also alter cellular homeostasis and cause internal damage, such as increased genomic instability. In this regard, we found several changes in *T. dohrnii* and *T. rubra* potentially affecting the molecular mechanisms that regulate the response to oxidative stress, such as the presence of five copies of *TXN* (thioredoxin) in *T. dohrnii*, as opposed to two in *T. rubra* (*SI Appendix*, section 3.3.5). Likewise, the glutathione reductase GSR appears to be duplicated in *T. dohrnii*, but not in *T. rubra* nor in the rest of the cnidarians analyzed in this work (*SI Appendix*, Table S4). Notably, we found that these genes were activated in *T. dohrnii* LCR (*SI Appendix*, Fig. S5) and previous studies have shown that their overexpression in *Drosophila melanogaster* resulted in an extension of their lifespan (15). In all, it is expected that genome stability and an appropriate redox status in cells from *T. dohrnii* are properly maintained. The expansion of these genes may confer this species protection against the accumulation of DNA damage due to both endogenous and exogenous factors.

Whereas the cnidarian telomeric sequence is shared with vertebrates (16), we found several variations in the telomerase and shelterin complexes in *T. dohrnii* in comparison to *T. rubra* and other cnidarians. These changes may contribute to a reduced telomere attrition and as a consequence to an enhanced cellular plasticity (*SI Appendix*, section 3.3.2). First, we found two copies of *GAR1* (ribonucleoprotein homolog) in the genome of *T. dohrnii*, while other cnidarians only have one copy of this gene. This result may indicate that telomerase activity could be enhanced or more finely regulated in this species. Regarding the shelterin complex, we found two different rare variants at the same position in POT1, p.G272N in *T. dohrnii* and p.G272R in *T. rubra* (*SI Appendix*, Table S5). This residue is highly conserved in metazoans, but a similar variant was found in *Chrysaora quinquecirrha* (Fig. 3), which suggests a case of parallel evolution (17).

To examine the functional impact of substitutions at these positions in POT1, we studied binding of recombinant human, *T. rubra* and *T. dohrnii* proteins to oligonucleotide probes containing three telomere-like repeats; the three variants were analyzed in each protein (G272, G272N, and G272R in humans and their equivalent positions in *Turritopsis* POT1) (Fig. 3). Wild-type POT1 presented the strongest affinity to the probes among human proteins, while binding decreased in the p.G272R mutant and was very weak in the p.G272N variant (Fig. 3*F*). These results confirm the functional relevance of residue at position 272 of POT1 in humans, which is consistent with the occurrence of several cancer-related variants and mutations in this residue (ClinVar IDs RCV001027221.1 and RCV000817038.3) (18). Importantly, *T. dohrnii* variant p.G272N dramatically reduced human POT1 binding to probes, suggesting an impact in its telomere-binding ability and, thus, in telomere maintenance. Given that POT1 binding to telomeres is necessary to achieve telomerase inhibition (19), the reduced affinity to DNA shown by both POT1 mutants may decrease this inhibitory effect. Notably, other variants affecting POT1, such as p.H266L or p.S322L, also decrease the ability of the protein to bind telomeres, which leads to telomere elongation (20). In *Turritopsis*, we did not observe the same binding differences as in humans, which could indicate that these residue modifications coevolved with other amino acid changes, thus generating epistatic modifications in POT1 (Fig. 3*F*). Interestingly, there is an apparent increase in affinity for *T. rubra* variants when compared with their wild-type counterpart. On the contrary, no telomere binding could be detected for any of the *T. dohrnii* proteins in the tested conditions. Therefore, the binding differences observed among *Turritopsis* might be more related to wider structural variations than just the abovementioned single residue changes (Fig. 3 *D* and *E*). Overall, our results hint toward a relevant role for maintenance of telomeres in rejuvenation of *T. dohrnii*. The linkage of telomeres and telomerase function with stem cell maintenance, DNA repair and aging (3) suggests that the telomere-related changes observed in *T. dohrnii* may be partially responsible for the enhanced cellular plasticity in this species.

Apart from telomere shortening and DNA damage, cellular senescence can also result from the deregulation of cell cycle (*SI Appendix*, section 3.3.6). In this regard, we found two exclusive variants of *T. dohrnii* in highly conserved residues of the serine/threonine kinase ataxia-telangiectasia mutated (ATM, p.P2553Y, and p.H2555Q, *SI Appendix*, Table S5 and Fig. S8). Both residues are located at the active site of this kinase whose activity leads to cell cycle arrest and induction of DNA repair. Furthermore, we also detected the presence of variants p.Q1362R and p.Q1362H in *T. dohrnii* and *T. rubra*, respectively, in a highly conserved residue of the ubiquitin ligase HECW2, which regulates the metaphase-to-anaphase transition during cell cycle and modulates the activity of p73 (*SI Appendix*, section 3.3.6 and Table S5 and Fig. S9).

Stem cell senescence and exhaustion can severely diminish the regenerative potential of tissues, which in turn contributes to organismal aging (3). In cnidarians, most genes related to pluripotency in vertebrates are missing, although some homologous genes may take over their function (21, 22). Using both automatic and manual annotation, we compared a set of relevant reprogramming genes and genes associated with differentiation pathways such as FOXO, HOX, WNT, JAK-STAT, and Hedgehog in cnidarians (*SI Appendix*, section 3.3.7 and Table S12). In this context, we found in *T. dohrnii* a duplication of *GLI3* (GLI family zinc finger 3), a gene encoding a transcription factor involved in Sonic hedgehog signaling. In contrast, *T. rubra* only exhibits a single *GLI3* copy, and this gene was absent in *H. vulgaris*, *C. hemisphaerica*, and *A. aurita*. In addition, all copies of *GLI3* were transcriptionally active during LCR of *T. dohrnii* (*SI Appendix*, Table S4 and Fig. S5). Altogether, these results suggest some improvement in the molecular mechanisms and pathways related to stem cell function in *T. dohrnii* compared to *T. rubra*.

Pathways related to intercellular communication, such as those regulating apoptosis, are particularly relevant during head regeneration of *H. vulgaris* (23, 24). Consistent with this, apoptosis has been reported in tissues from *T. dohrnii* during LCR (25). In this regard, we found gene amplifications associated with the neural system and apoptosis such as a duplication in *PSEN1* (presenilin 1) in *T. dohrnii* compared to a single copy in *T. rubra*, as well as a notable expansion of *BMP7* (bone morphogenetic protein 7), a gene with pleiotropic effects in

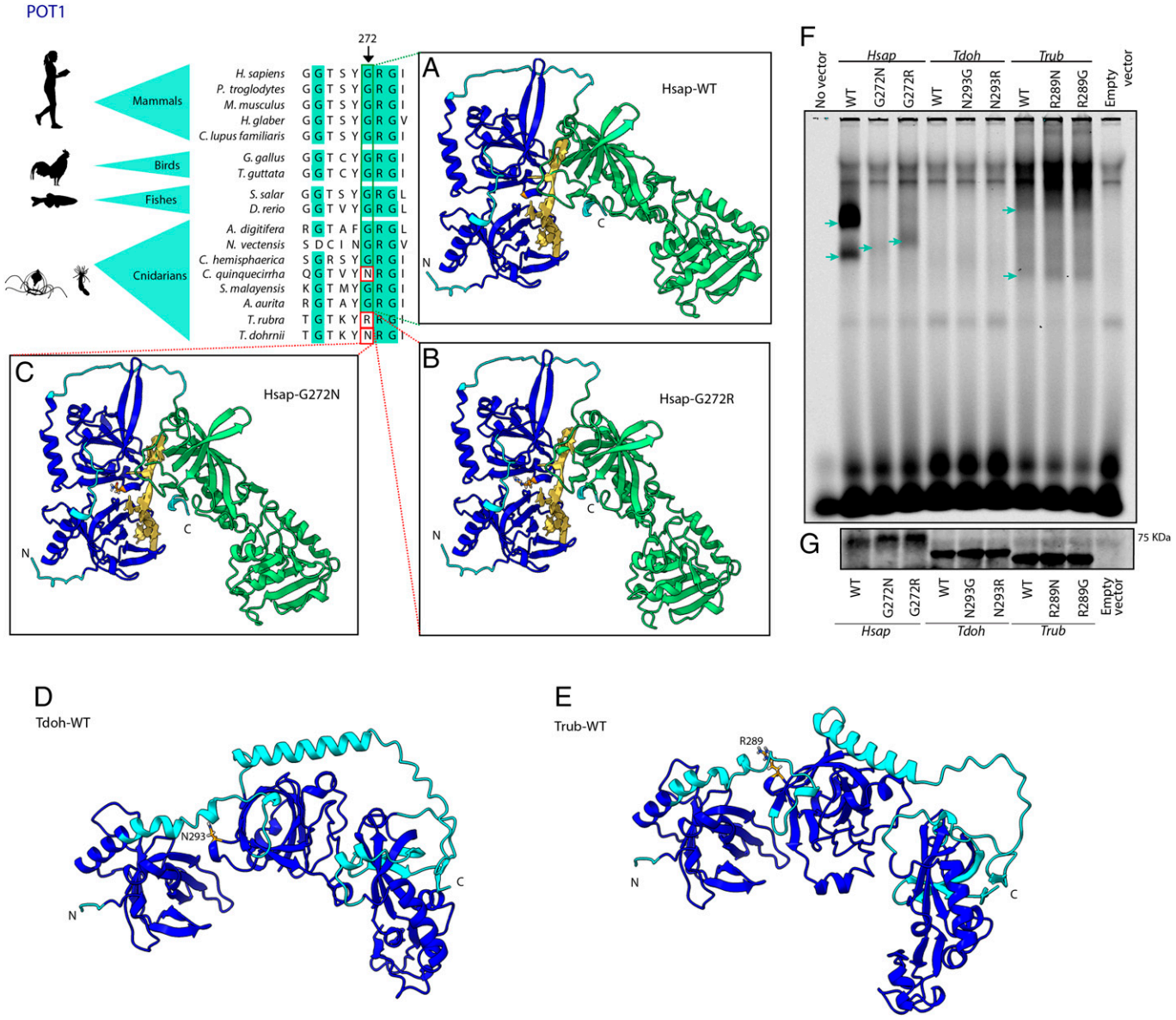

Fig. 3. Structural and functional comparisons between POT1 from *Turritopsis* and other species. The figure shows a partial amino acid sequence alignment of POT1 from *Turritopsis* and other cnidarians, invertebrates and vertebrate species. Significant variants in *T. dohrnii* and *T. rubra* are highlighted with a red box and the arrow indicates the specific position. The figure also shows protein structures built with AlphaFold using *H. sapiens* structure (*A*) wild-type, (*B*) with *T. rubra*, and (*C*) *T. dohrnii* variants, and using (*D*) *T. dohrnii* and (*E*) *T. rubra* wild-types. Dark blue surface indicates oligonucleotide binding fold (OBF) domain which binds to ssDNA and green area represents OB-fold domain and a Holliday junction resolvase (HJR) domain which make dimer contacts with TPP1. Yellow structure is a tentative representation of the telomeric region, located by superimposing POT1-telomere model (PDB ID 1XJV) on each AlphaFold model. (*F*) Binding of the different POT1 variants to a single-stranded oligonucleotide containing three telomeric repeats. Blue arrows point to POT1-$(TTAGGG)_3$ complexes (*G*) Western blot to check the amount of POT1 loaded in the binding assay.

modulation of apoptosis (26, 27). *BMP7* had eight copies in *T. dohrnii* (five of them found to be active during LCR), in contrast to five copies in *T. rubra* and three copies in *H. vulgaris* (*SI Appendix*, Table S4). Interestingly, although none of the other genes related to apoptosis showed differential amplifications in *T. dohrnii* (*SI Appendix*, Table S13), we did find a clear overexpression of one copy of *CASP3* (caspase 3), *BCL2* (B-cell lymphoma 2), and *BAX* (Bcl2-associated X) during LCR (from postincubation to late stolon) (*SI Appendix*, Fig. S5). Finally, we detected gene amplifications that could impact microtubule regulation, which in turn could enhance neuronal function and cell plasticity (28). Specifically, *T. dohrnii* showed duplications of *TUBG1* (tubulin gamma 1), *CLASP1* (cytoplasmic linker associated protein 1), and *SPAST* (spastin) (all transcriptionally active during LCR), compared to *T. rubra* and the rest of cnidarian species analyzed in this work (*SI Appendix*, Table S4).

Proper regulation of transcriptional patterns and epigenetic modifications is also essential for the maintenance of an appropriate cellular function. Through detailed analysis of genes involved in transcriptional and posttranscriptional regulation, we detected copy number variations affecting genes such as *MORC3* (microrchidia 3), that can act as a chromatin-binding modulator (29), with four copies in *T. dohrnii*, while other cnidarians have at most three copies of this gene (*SI Appendix*, section 3.3.3 and Table S4). Deficient transcriptional regulation can also lead to loss of proteostasis, another major hallmark of aging (3). In this context, we found the presence of the variant p.V518I in the calcium binding site of TPP1

(tripeptidyl peptidase 1) in *T. dohrnii* (*SI Appendix*, section 3.3.4 and Table S5 and Fig. S7). Notably, deficiencies in this peptidase cause neuronal ceroid lipofuscinosis (30).

As a whole, functionality of genes highlighted in this genome comparison is supported by expression analysis during LCR of *T. dohrnii* (*SI Appendix*, Fig. S5). Most differential genes involved in maintaining genome stability (*POLD1*, *POLA2*, *XRCC5*, and *MSH2*) and those related to telomere maintenance (*POT1*, *GAR1*) were underexpressed from reduction phase to late stolon, from which they increased the expression, suggesting that replicative and postreplicative repair systems and telomere maintenance activities could follow the same pattern. Genes aimed at keeping redox environment were overexpressed at different stages (*TXN* from incubation to early stolon and *GSR* from late stolon to mature polyp), whereas those associated with cell senescence (*RACGAP1* and *SPICE1*), that regulate different phases of the cell cycle, were underexpressed from cyst to polyp formation. In contrast, *HECW2* was overexpressed throughout the process, suggesting that this ubiquitin ligase could be regulating p73 activity rather than metaphase/anaphase transition. *GLI3*, associated with stem cell maintenance and differentiation, was activated from reduction phase to mature polyp, and *PSEN1* could strengthen cellular communication during the first period of LCR (from incubation to cyst), likely improving organismal regulation.

After the detailed gene annotation of *Turritopsis* genomes and the expression analysis of specific genes highlighted after genomic comparisons between *T. dohrnii* and *T. rubra*, we examined the LCR transcriptome of *T. dohrnii* to address whether cell reprogramming takes place and, if so, which molecular pathways are implicated. Gene set enrichment analysis (GSEA) highlighted pathways related to polycomb repression complex 2 (PRC2) targets and pluripotency related genes (Fig. 4 and *SI Appendix*, Table S15), both necessary for promoting dedifferentiation (31). Firstly, PRC2 catalyzes trimethylation of histone 3 Lys-27 (H3K27), silencing a specific set of genes involved in development, which is necessary for enhancing and maintaining pluripotency in embryonic stem cells (32). The underexpression of this gene set, previously undescribed in jellyfish, was especially notorious during the cyst stage (Fig. 4 and *SI Appendix*, section 3.4.2 and Fig. S10). Interestingly, we did not find any clear overexpression of PRC2 components or its associated proteins, in contrast with studies of transdifferentiation in *Podocoryne carnea* and in *H. vulgaris* (33, 34). These results suggest that PRC2

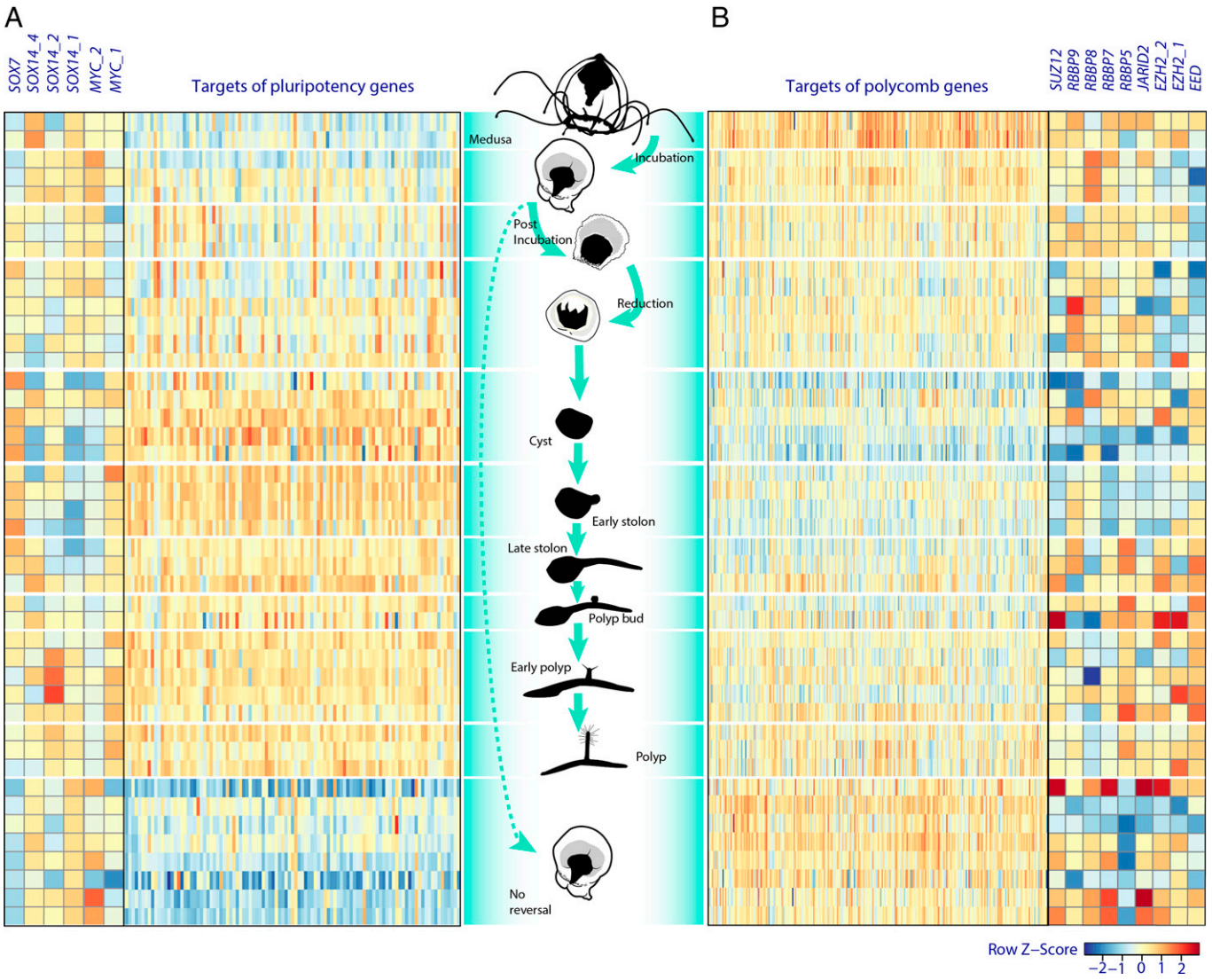

Fig. 4. Heatmap of pluripotency targets (NANOG, OCT4, SOX2, and MYC targets) (*A*) and PRC2 targets (*B*) during LCR of *T. dohrnii*. The figure also shows the expression of genes potentially inducing pluripotency (*Left*) and genes coding for the PRC2 components (*Right*). Note that heatmap "A" only includes targets of pluripotency genes whose expression in any stage from incubation to polyp was clearly different from their expression in medusa and in no reversal stages.

regulation in *T. dohrnii* could be occurring at the protein level. Secondly, in the gene set associated with pluripotency that was differentially expressed in the cyst and early stolon stages, most of the overexpressed genes were related to protein homeostasis, but also involved in oxidative stress resistance, DNA replication, DNA repair, and apoptosis (*SI Appendix*, section 3.4.3 and Fig. S11). We found that only *SOX7* (SRY-box transcription factor 7), *SOX14* (SRY-box transcription factor 14) and two copies of *MYC* (Myc proto-oncogene protein) exhibit a differential pattern during LCR of *T. dohnrii*. *Sox7* has not been previously related to pluripotency in cnidarians, but it has been reported that this transcription factor can gain reprogramming activity when a single amino acid residue of its structure is modified in mouse fibroblasts (35). Moreover, one of the *SOX14* (*SOX14_1*) copies was clearly underexpressed during the same stages as *SOX7*, which could affect cell commitment from cyst to late stolon since expression of *SOX14* has been associated with cell differentiation in *C. hemisphaerica* (35). Finally, *MYC_1* was overexpressed from incubation to reduction stage and *MYC_2* from cyst to mature polyp (Fig. 4). Therefore, both *MYC*-like genes may exhibit nonredundant functions during LCR as described in *H. vulgaris*, where *MYC1* is associated with cell cycle and ribosome biogenesis and *MYC2* with activation of gamete production in epithelial interstitial stem cells (22, 36).

In summary, the draft genomes of the immortal *T. dohrnii* and its mortal congeneric species, *T. rubra*, highlight candidate genes and pathways related to genomic instability, telomere attrition, mitochondrial dysfunction, stem cell exhaustion, cellular senescence, and intercellular communication. Specifically, our results suggest that gene amplification and point variants unique of *T. dohrnii* could affect its replicative efficiency, as well as DNA repair and telomere maintenance activity, which may be pivotal processes for cell rejuvenation and proliferation. In addition, expansions and sequence variations of genes associated with DNA repair, mitochondrial dysfunction and intercellular communication could increase its capacity to maintain redox environment and reduce cellular damage during stress events. Furthermore, regulation of cellular senescence in terms of cell cycle control could strengthen plasticity and regeneration capacities in both *Turritopsis* species. Finally, we have found that two of the main mechanisms for cell reprogramming, silencing of PRC2 targets and activation of pluripotency targets, are involved in *T. dohrnii* LCR, which leads us to propose these factors as suitable candidates to mediate the activation of pluripotency signaling. Altogether, this work provides insights into the molecular mechanisms giving *T. dohrnii* the remarkable capacity to rejuvenate and escape death.

Materials and Methods

Genome Sequencing and Assembly. We obtained DNA of *T. dohrnii* from specimens collected in Santa Caterina, Lecce, Italy, and of *T. rubra* from the north of Hokkaido Island, Japan (through Blue Corner Inc.), using a standard phenol-chloroform extraction protocol. Samples from both *Turritopsis* species were sequenced and assembled through Macrogen commercial services, using Illumina platform, from a 150 bp pair-end library (Truseq DNA PCR-free, 350 bp), and Platanus-allee (v2.2.2) (37) and Platanus (v1.2.4) (38) for *T. dohrnii* and *T. rubra*, respectively, considering the differences in heterozygosity found among these species. Total RNA was extracted from *T. dohrnii* using TRIzol reagent (Invitrogen), retrotranscribed to cDNA with the SMARTer Ultra Low Input RNA Kit, used to construct a 150 bp pair-end library and sequenced by Novogene Co., Ltd. Total RNA in *T. rubra* was extracted with a combination of TRIzol reagent and RNAeasy Mini Kit columns (Qiagen), and sequenced by Macrogen commercial services. These RNA-seq reads were used for automatic annotation, validation of gene variants and for further transcriptomic analysis of LCR of *T. dohrnii* (*SI Appendix*, sections 2.1 and 2.2).

Genome Annotation. Using the genome assembly and RNA-seq data of *T. dohrnii*, together with curated protein sequences from human, freshwater hydra, *Aurelia* and other Cnidaria, we performed de novo annotation with MAKER (39) with three successive runs in a Microsoft Azure virtual machine. In parallel, we used selected genes from the human protein database in Ensembl as a reference to manually predict the corresponding homologs in the genomes of *Turritopsis* species by using the BATI algorithm (Blast, Annotate, Tune, Iterate) (40). This algorithm allows users to annotate the position and intron/exon boundaries of Tblastn results, retrieving more accurate results. This procedure also facilitates the detection of novel homologs.

***POT1 In vitro* Translation and Telomeric G-Strand Binding Assay.** Codon-optimized wild-types of human, *T. dohrnii*, and *T. rubra POT1*, and their respective modified forms (with a Gly, Asn, or Arg residues) were generated using gene synthesis by GenScript and cloned as C-ter-FLAG tagged proteins in a pCDNA3.1 expression vector. These vectors were used for protein production by in vitro translation using the TNT coupled reticulocyte lysate kit (Promega) following manufacturer's instructions. In brief, 25 μL reaction mixtures containing 0.5 μg of plasmid DNA and 24 μL of rabbit reticulocyte translation reaction mix were incubated at 30 °C for 90 min. Five microliter fractions of each reaction were used to assess protein translation by sodium dodecyl sulfate-polyacrylamide gel electrophoresis (SDS-PAGE) followed by immunoblotting with a rabbit anti-DYKDDDDK Tag Antibody (Cell Signaling). DNA binding assays were performed in 20 μL reaction mixtures, by incubating 15 μL of each respective translation reaction product (and 5 μL only in case of human POT1 *wild-type*) with 2 μL of 100 nM of a fluorescently labeled telomeric oligonucleotide (IR800-GGTTAGGGT TAGGGTTAGGGTTAGGGTTAGGG) and 1 μg of the nonspecific competitor DNA poly [dI-dC] in binding buffer (25 mM Hepes-NaOH, pH 7.5, 100 mM NaCl, 1 mM ethylenediaminetetraacetic acid (EDTA), and 5% glycerol). After 30 min of incubation at room temperature, protein-DNA complexes were analyzed by electrophoresis on a 6% polyacrylamide Tris-borate EDTA gel, which was run at 160 V for 4 h. Gels were further visualized using an Odyssey Infrared Imaging System (Li-Cor Biosciences).

Alphafold Protein Structure Prediction. Structural prediction of POT1 in *T. dohrnii* and *T. rubra* was performed, alongside with its *wild-type* human ortholog POT1 and its variants (G272R and G272N), by using the AlphaFold v.2.1.2 pipeline (https://github.com/deepmind/alphafold/). We performed the pipeline with the monomer preset and full databases, and then used the structure with the highest confidence score (pLDDT) for later analysis. Structure with the highest confidence score was tuned until final protein structure using ChimeraX (41) and information from previous studies of POT1 structure (42, 43).

LCR Experiment and RNAseq Analyses. Ontogeny reversal of *T. dohrnii* was triggered by incubating 1-d starved medusae in 116 mM CsCl for 5 h. Several samples were taken individually in each stage of the process (medusa, incubation, postincubation, reduction phase, cyst, early stolon formation, late stolon, bud formation, early polyp, and polyp) and were frozen immediately until RNA extraction. STAR (44) was used for aligning RNA sequences of each sample to the assembled *T. dohrnii* genome and edgeR (45) and *limma* (46) for modeling differential expression between stages, after applying *voom* (47) transformation to consider library size variability. GSEA was performed with the *fgsea* (48) package, after adapting the human Molecular Signatures Database (MSigDB) (49) to the genome of *T. dohrnii*. Libraries with less than two million reads and low-expression genes were excluded from the analysis. Differentially expressed genes and enriched pathways were identified based on a false-discovery rate adjusted *P* value of 0.05.

Data, Materials, and Software Availability. Sequencing data have been deposited at the Sequence Read Archive (SRA, https://www.ncbi.nlm.nih.gov/sra), and the MAKER2 predicted protein sequences can be downloaded from https://github.com/vqf/turritopsis (50). Assemblies are hosted by the National Center for Biotechnology Information (NCBI, https://www.ncbi.nlm.nih.gov/), under accession number (JAIFHF000000000 for *T. dohrnii* and JAHXJM000000000 for *T. rubra*) for SRA sequences, and BioProject PRJNA734867 (51) for GenBank submissions.

ACKNOWLEDGMENTS. We thank Susana Acle and Bioparc Acuario de Gijón for their support and suggestions in aquaria maintenance, and all members of

the Medusas's group (ICM-CSIC) for their help in setting up the first jellyfish cultures. We also thank Cetarea El Musel, Servicio de Patrimonio (Universidad de Oviedo) and Neoalgae (especially to David Suárez) for facilitating the sea water supply for jellyfish maintenance and experiments. Particular thanks also to Xose S. Puente, José M. P. Freije, Alicia R. Folgueras and Alejandro P. Ugalde for their helpful advice and comments, and Tomàs Marquès-Bonet, Lukas F.K. Kuderna and Aitor Serres-Armero for their expert recommendations in genome assembly. This work was supported by European Research Council (DeAge, ERC Advanced Grant, 742067) and the Ministerio de Ciencia e Innovación-FEDER (SAF2017-87655-R; PID2020-118394RB-I00; RTI2018-096859-B-I00). This work was also a contribution of the Observatorio Marino de Asturias.

[a]Departamento de Bioquímica y Biología Molecular, Instituto Universitario de Oncología, Ciberonc, Universidad de Oviedo, Oviedo, 33006, Spain; [b]Observatorio Marino de Asturias, Departamento de Biología de Organismos y Sistemas, Universidad de Oviedo, Oviedo, 33006, Spain; [c]Departamento de Biología Funcional, Facultad de Medicina, Universidad de Oviedo, Oviedo, 33006, Spain; and [d]Autophagy and Metabolism Lab, Instituto de Investigación Sanitaria del Principado de Asturias (ISPA), Oviedo, 33011, Spain

Author contributions: M.P.-T. and C.L.-O. designed research; M.P.-T., D.C., J.G.P-S., D.Á.-P., D.R.-V., G.B., D.R., D.M. performed research; M.P.-T., D.C., J.G.P.-S., D.Á.-P., and D.R.-V. analyzed data; M.P.-T. and D.C. wrote the paper; M.P.-T. field sample collection and sampling, culture maintenance, and LCR experiments; D.Á.-P. culture maintenance and LCR experiments; D.R.-V. protein modeling; G.B., D.R., and D.M. carried out functional studies; E.M.-G. field sample collection; Y.E. project planning and supervision; G.M. first conceived the study; J.L.A. supervised the logistics of *T. dohrnii* cultures; V.Q. supervised bioinformatic analyses; and C.L.-O. first conceived the study and supervised the whole research.

1. T. Flatt, P. S. Schmidt, Integrating evolutionary and molecular genetics of aging. *Biochim. Biophys. Acta* **1790**, 951–962 (2009).
2. C. López-Otín, G. Kroemer, Hallmarks of health. *Cell* **184**, 1929–1939 (2021).
3. C. López-Otín, M. A. Blasco, L. Partridge, M. Serrano, G. Kroemer, The hallmarks of aging. *Cell* **153**, 1194–1217 (2013).
4. N. H. Putnam *et al.*, Sea anemone genome reveals ancestral eumetazoan gene repertoire and genomic organization. *Science* **317**, 86–94 (2007).
5. J. A. Chapman *et al.*, The dynamic genome of Hydra. *Nature* **464**, 592–596 (2010).
6. D. A. Gold *et al.*, The genome of the jellyfish Aurelia and the evolution of animal complexity. *Nat. Ecol. Evol.* **3**, 96–104 (2019).
7. D. De Vito, S. Piraino, J. Schmich, J. Bouillon, F. Boero, Evidence of reverse development in Leptomedusae (Cnidaria, Hydrozoa): The case of *Laodicea undulata* (Forbes and Goodsir 1851). *Mar. Biol.* **149**, 339–346 (2006).
8. V. Schmid, M. Wydler, H. Alder, Transdifferentiation and regeneration in vitro. *Dev. Biol.* **92**, 476–488 (1982).
9. J.-Y. Li, D.-H. Guo, P.-C. Wu, L.-S. He, Ontogeny reversal and phylogenetic analysis of *Turritopsis* sp.5 (Cnidaria, Hydrozoa, Oceaniidae), a possible new species endemic to Xiamen, China. *PeerJ* **6**, e4225 (2018).
10. S. Piraino, F. Boero, B. Aeschbach, V. Schmid, Reversing the life cycle: Medusae transforming into polyps and cell transdifferentiation in *Turritopsis nutricula* (Cnidaria, Hydrozoa). *Biol. Bull.* **190**, 302–312 (1996).
11. Y. Matsumoto, S. Piraino, M. P. Miglietta, Transcriptome characterization of reverse development in *Turritopsis dohrnii* (Hydrozoa, Cnidaria). *G3 (Bethesda)* **9**, 4127–4138 (2019).
12. K. Adachi, H. Miyake, T. Kuramochi, K. Mizusawa, Genome size distribution in phylum Cnidaria. *Fish. Sci.* **83**, 107–112 (2017).
13. V. Quesada *et al.*, Giant tortoise genomes provide insights into longevity and age-related disease. *Nat. Ecol. Evol.* **3**, 87–95 (2019).
14. D. Carrero, J. G. Pérez-Silva, V. Quesada, C. López-Otín, Differential mechanisms of tolerance to extreme environmental conditions in tardigrades. *Sci. Rep.* **9**, 14938 (2019).
15. Y. Umeda-Kameyama *et al.*, Thioredoxin suppresses Parkin-associated endothelin receptor-like receptor-induced neurotoxicity and extends longevity in *Drosophila*. *J. Biol. Chem.* **282**, 11180–11187 (2007).
16. M. C. Ojimi, N. Isomura, M. Hidaka, Telomerase activity is not related to life history stage in the jellyfish *Cassiopea* sp. *Comp. Biochem. Physiol. A Mol. Integr. Physiol.* **152**, 240–244 (2009).
17. J. F. Storz, Causes of molecular convergence and parallelism in protein evolution. *Nat. Rev. Genet.* **17**, 239–250 (2016).
18. C. D. Robles-Espinoza *et al.*, POT1 loss-of-function variants predispose to familial melanoma. *Nat. Genet.* **46**, 478–481 (2014).
19. C. Kelleher, I. Kurth, J. Lingner, Human protection of telomeres 1 (POT1) is a negative regulator of telomerase activity in vitro. *Mol. Cell. Biol.* **25**, 808–818 (2005).
20. H. Takai *et al.*, A POT1 mutation implicates defective telomere end fill-in and telomere truncations in Coats plus. *Genes Dev.* **30**, 812–826 (2016).
21. R. C. Millane *et al.*, Induced stem cell neoplasia in a cnidarian by ectopic expression of a POU domain transcription factor. *Development* **138**, 2429–2439 (2011).
22. D. A. Gold, D. K. Jacobs, Stem cell dynamics in Cnidaria: Are there unifying principles? *Dev. Genes Evol.* **223**, 53–66 (2013).
23. H. Watanabe, T. Fujisawa, T. W. Holstein, Cnidarians and the evolutionary origin of the nervous system. *Dev. Growth Differ.* **51**, 167–183 (2009).
24. S. Chera *et al.*, Apoptotic cells provide an unexpected source of Wnt3 signaling to drive hydra head regeneration. *Dev. Cell* **17**, 279–289 (2009).
25. E. C. Carla', P. Pagliara, S. Piraino, F. Boero, L. Dini, Morphological and ultrastructural analysis of *Turritopsis nutricula* during life cycle reversal. *Tissue Cell* **35**, 213–222 (2003).
26. A. Segklia *et al.*, Bmp7 regulates the survival, proliferation, and neurogenic properties of neural progenitor cells during corticogenesis in the mouse. *PLoS One* **7**, e34088 (2012).
27. L. K. Bollum *et al.*, BMP-7 induces apoptosis in human germinal center B cells and is influenced by TGF-β receptor type I ALK5. *PLoS One* **12**, e0177188 (2017).
28. C. E. Fogarty, A. Bergmann, Killers creating new life: Caspases drive apoptosis-induced proliferation in tissue repair and disease. *Cell Death Differ.* **24**, 1390–1400 (2017).
29. A. Rosendorff *et al.*, NXP-2 association with SUMO-2 depends on lysines required for transcriptional repression. *Proc. Natl. Acad. Sci. U.S.A.* **103**, 5308–5313 (2006).
30. L. Ma, A. M. Prada, M. Schmidt, E. M. Morrow, Generation of pathogenic TPP1 mutations in human stem cells as a model for neuronal ceroid lipofuscinosis type 2 disease. *Stem Cell Res. (Amst.)* **53**, 102323 (2021).
31. K. Takahashi, S. Yamanaka, A decade of transcription factor-mediated reprogramming to pluripotency. *Nat. Rev. Mol. Cell Biol.* **17**, 183–193 (2016).
32. S. Girirajan *et al.*, Tom1l2 hypomorphic mice exhibit increased incidence of infections and tumors and abnormal immunologic response. *Mamm. Genome* **19**, 246–262 (2008).
33. R. Lichtneckert, P. Müller, V. Schmid, S. Reber-Müller, Evolutionary conservation of the chromatin modulator Polycomb in the jellyfish *Podocoryne carnea*. *Differentiation* **70**, 422–428 (2002).
34. G. Genikhovich, U. Kürn, G. Hemmrich, T. C. G. Bosch, Discovery of genes expressed in Hydra embryogenesis. *Dev. Biol.* **289**, 466–481 (2006).
35. M. Jager, E. Quéinnec, H. Le Guyader, M. Manuel, Multiple Sox genes are expressed in stem cells or in differentiating neuro-sensory cells in the hydrozoan *Clytia hemisphaerica*. *Evodevo* **2**, 12 (2011).
36. M. Hartl *et al.*, Stem cell-specific activation of an ancestral myc protooncogene with conserved basic functions in the early metazoan Hydra. *Proc. Natl. Acad. Sci. U.S.A.* **107**, 4051–4056 (2010).
37. R. Kajitani *et al.*, Platanus-allee is a de novo haplotype assembler enabling a comprehensive access to divergent heterozygous regions. *Nat. Commun.* **10**, 1702 (2019).
38. R. Kajitani *et al.*, Efficient de novo assembly of highly heterozygous genomes from whole-genome shotgun short reads. *Genome Res.* **24**, 1384–1395 (2014).
39. M. S. Campbell, C. Holt, B. Moore, M. Yandell, Genome annotation and curation using MAKER and MAKER-P. *Curr. Protoc. Bioinformatics* **48**, 4.11.1–4.11.39 (2014).
40. V. Quesada, G. Velasco, X. S. Puente, W. C. Warren, C. López-Otín, Comparative genomic analysis of the zebra finch degradome provides new insights into evolution of proteases in birds and mammals. *BMC Genomics* **11**, 220 (2010).
41. E. F. Pettersen *et al.*, UCSF ChimeraX: Structure visualization for researchers, educators, and developers. *Protein Sci.* **30**, 70–82 (2021).
42. M. Lei, E. R. Podell, T. R. Cech, Structure of human POT1 bound to telomeric single-stranded DNA provides a model for chromosome end-protection. *Nat. Struct. Mol. Biol.* **11**, 1223–1229 (2004).
43. C. Chen *et al.*, Structural insights into POT1-TPP1 interaction and POT1 C-terminal mutations in human cancer. *Nat. Commun.* **8**, 14929 (2017).
44. A. Dobin *et al.*, STAR: Ultrafast universal RNA-seq aligner. *Bioinformatics* **29**, 15–21 (2013).
45. M. D. Robinson, D. J. McCarthy, G. K. Smyth, edgeR: A Bioconductor package for differential expression analysis of digital gene expression data. *Bioinformatics* **26**, 139–140 (2010).
46. M. E. Ritchie *et al.*, limma powers differential expression analyses for RNA-sequencing and microarray studies. *Nucleic Acids Res.* **43**, e47 (2015).
47. C. W. Law, Y. Chen, W. Shi, G. K. Smyth, voom: Precision weights unlock linear model analysis tools for RNA-seq read counts. *Genome Biol.* **15**, R29 (2014).
48. G. Korotkevich *et al.*, Fast gene set enrichment analysis. bioRxiv [Preprint] (2021). 10.1101/060012. Accessed 28 May 2021.
49. A. Liberzon *et al.*, Molecular signatures database (MSigDB) 3.0. *Bioinformatics* **27**, 1739–1740 (2011).
50. M. Pascual-Torner *et al.*, Comparative genomics of mortal and immortal cnidarians unveils novel keys behind rejuvenation. GITHUB. https://github.com/vqf/turritopsis. Deposited 28 May 2021.
51. M. Pascual-Torner *et al.*, Comparative genomics of mortal and immortal cnidarians unveils novel keys behind rejuvenation. BioProject. https://www.ncbi.nlm.nih.gov/sra/PRJNA734867. Deposited 28 May 2021.